Interactive comment on "Theoretical framework for estimating snow distribution through point measurements" by E. Trujillo and M. Lehning

Anonymous Referee #1

Received and published: 29 January 2015

This paper presents estimators for errors of point snow measurements relative to the true mean along transects and within specified areas. Estimators of how representative point measurements are in space are an important topic that so far has received little attention in snow research. The authors assume that snow depth is a random field that exhibits spatial correlation according to an exponential model. From this assumption they estimate the errors by integrating the random variable along transects (1D) and over specified areas (2D).

As far as I can see the derivations are correct.

However, I have difficulties with the way the material is presented. The title suggests that the paper proposes a framework. I do not think this is the case. Instead the paper uses standard geostatistical methods and compares them with snow data. The equations are presented as if they were new, as no references are given. This is misleading as they have been developed by Matheron and colleagues more than half a century ago and can be found in geostatistical textbooks (see eg. Journel and Huijbregts pp. 84 and 117 for the 1D and 2D cases, respectively).

Response: *We would like to thank the reviewer for his/her useful comments; they have led to a more clarified introduction, overall presentation of methods and results and an improved discussion. We thank the reviewer for pointing out the reference and the need to acknowledge the previous work in this area, which was not known to us. The references to the works by Matheron and subsequent examples are now included.*

I also have difficulties with the notion that the estimators are specific to snow or hydrologically-relevant variables (p. 24). They apply to ANY random field that is correlated according to an exponential model.

RE: *We agree with the reviewer on this point, which is why we refer to the other hydrologic variables as examples in the original manuscript. We have added clarification to this in the Introduction more explicitly in the resubmission to be more emphatic about this.*

Also, in response to both of these main comments, we have tried to clarify these points in the article from the beginning, as it is not our intention to claim to be the proposers of the first principles of geostatistics that our approach is based on. We have tried to make even more clear and explicit that the motivations of this study are based on what we see as lacking in snow sciences even in the present. Also, we have added references to the researchers and authors that have made contributions in such geostatistical approaches to give appropriate credit. And let us also point out that the derivations are presented for the understanding of the snow community, as so far there have been no examples of these approaches in snow sciences to our knowledge. Evidence of this are the comments by the second reviewer, who suggested the addition of more details about some of the geostatistical principles behind the derivation.

The following changes are suggested:

Change title to something like: "Geostatistical estimation of point measurement errors

- comparisons with snow data"

RE: *We have given thorough consideration to the reviewer's suggestion regarding the title. We have changed the title to "Theoretical Analysis of Errors when Estimating Snow*

Distribution through Point Measurements" in response to the reviewers suggestion.

Make it clear that the method is known (and has been known for a long time in fact) and is applied to snow data in this paper. The new contributions of the paper are the comparisons with the snow data but certainly not the equations. Give full credit to the geostatistical literature when presenting the equations and the plots where their numerical values are shown.

RE: *Although we were not aware of any derivations that are identical to our equations, the literature the referee has pointed out to us shows a similar approach and is now acknowledged. References to Matheron, Journel and Hiujbregts have been added.*

Also say that the kind of variable does not matter in this approach as the variable is fully specified by its variance and correlation scale.

RE: *As indicated above, we have now added explicit clarification to this in the Introduction.*

Discuss in more detail what makes the snow application interesting. The cryospheric aspects in the current paper are limited to the shape of the covariance function. For example, it would be of interest how the correlation scale is related to the snow physical characteristics.

RE: *In the resubmission, we have added in the Introduction, and Summary and Discussions more explicit reference to how this is mainly directed to snow variables, and how the methodology can be used for the particular case of snow depth and other snow related variables, such as SWE. Discussions of the correlation lengths in snow depth and their relashionships to the physical processes have been presented in previous studies, which are referenced throughout the article where appropriate (e.g., Trujillo et al., 2007; Deems et al., 2008; Trujillo et al., 2009).*

With these changes, the paper will be an interesting application of geostatistics to the snow sampling case.

References

Journel, A. G. and Huijbregts, C.J. (1978) Mining Geostatistics, Academic Press

References

Deems, J. S., Fassnacht, S. R., and Elder, K. J.: Interannual Consistency in Fractal Snow Depth Patterns at Two Colorado Mountain Sites, *J. Hydrometeor., 9*(5), 977-988, doi: 10.1175/2008jhm901.1, 2008.

Trujillo, E., Ramirez, J. A., and Elder, K. J.: Topographic, meteorologic, and canopy controls on the scaling characteristics of the spatial distribution of snow depth fields, *Water Resour. Res., 43*, W07409, doi: 10.1029/2006WR005317, 2007.

Trujillo, E., Ramírez, J. A., and Elder, K. J.: Scaling properties and spatial organization of snow depth fields in sub-alpine forest and alpine tundra, *Hydrol. Processes, 23*, 1575–1590, doi: 10.1002/hyp.7270, 2009.

Interactive comment on "Theoretical framework for estimating snow distribution through point measurements" by E. Trujillo and M. Lehning

Anonymous Referee #2

Received and published: 15 February 2015

Trujillo and Lehning present a theoretical model for quantifying errors/uncertainty in snow measurements (in this case snow depth) and demonstrate the validity of the model using LiDAR data from the CLPX project (Colorado, USA) at a forested site and at a wind-influenced area. This work provides an important contribution to snow science, as there has been minimal attention to errors associated with the design of snow surveys. To my knowledge, the framework appears to have no technical issues.

The authors apply it for a number of different examples that will be of interest to snow field studies. I recommend for publication in The Cryosphere after attention to a suite of (mostly minor) comments below.

Response: *We would like to thank the reviewer for his insightful and encouraging comments. We hope to clarify all concerns and address all suggestions below. The suggestions have been very useful to improve the quality of the revised manuscript.*

GENERAL COMMENTS

- The mathematical framework is likely to be new material to some snow scientists, so I would argue that additional citations and an expanded background section should be included to provide resources for learning about the methodological framework. I suspect some may be unfamiliar with first/second order stationary processes, and most equations (after equation 3) may not be obvious to all readers. This would help to maximize comprehension of the theoretical framework.

Response: *Thank you, we have now added some additional explicit clarification/references in the Background section where appropriate in response to this comment and the recommendations from Reviewer 1. The original manuscript refers to the main implications of first and second order stationarity where the assumption is mentioned in the section, and we have added references to textbooks where the concept is fully explained. Also, we have included reference to this assumption in the "Summary and Conclusions" section (see response to first Specific Comment). The new references are:*

Journel, A. G. and C. J. Huijbregts (1978). Mining Geostatistics. Academic Press, London.

Cressie, N. (1993). Statistics for spatial data. John Wiley & Sons, Inc, USA.

- The study was conducted with LiDAR data near peak snow conditions (assuming nearly full snow cover). How might the analysis and the theoretical framework change in a situation with patchy or incomplete snow cover, such as during the middle of the snowmelt season? Please discuss.

RE: *Let us point out that the methodology is not really suitable for patchy/discontinuous snow covers because the spatial probability distribution of snow depth (and SWE for that matter) would now take the form of a truncated distribution with a discrete non-zero probability (or density if probability density function) at zero equal to the area with no snow cover. Such situation requires a different approach in*

which, for example, samples from the areas with no snow covered can be considered as censored samples, and as such would need a different development not considered here. It is however an interesting question, but not addressed in the context of this article. We added a discussion to this in the "Summary and Conclusions" of the revised manuscript.

SPECIFIC COMMENTS

- The development of the framework (section 2) would be better supported if the authors cited prior works that demonstrate snow distributions can be approximated as 1st or 2nd order stationary processes and with exponential decay (hence providing the basis for their hypothesis in the theoretical framework).

RE: *Unfortunately, there are not many examples that refer to this in the context of snow distribution in the literature, but we have added some text to discuss this approximation in the "Summary and Conclusions" section of the revised manuscript. The text reads:*

"Here, we should highlight some of the implications of the assumptions made in the model. In simplified terms, the second-order stationarity assumption implies that the mean and the variance of the process/variable (e.g., snow depth) are independent of the spatial location, and that the covariance is dependent only on the separation vector (i.e., lag). Although these assumptions may not be as adequate over larger scales (e.g., greater than 100 m), at smaller scales the assumption in the context of the model application to snow depth should be valid. We present these examples to show how the error can be quantified with good accuracy around such smaller scales. Application of such types of approaches at larger scales will require additional evaluations with particular attention as to what the specific demands of the application are".

- Does the theoretical model match the observations only because the exponential decay exponent was fitted to the data (e.g., page 14, lines 2-7)? Were independent data used to fit the exponent? If not, then there is a problem here where the same LiDAR data are used for both fitting and for model evaluation. Please clarify and rectify this issue.

RE: *The model requires prior assumption of a correlation/covariance model and estimates of the parameters of this model (e.g., the decay exponent for the exponential case). In the implementation we indeed use the LIDAR data for the parameter estimation, which we have done to illustrate the applicability of the model and its ability to estimate the error using real snow depth data. We have added a discussion of this in the "Summary and Conclusions" section. We clarify how the model can be implemented if prior information is not available, which directly addresses this comment. And to help clarify why this implementation is possible, we would like to make the following remarks that support the applicability of the model for snow depth:*

1) The sensitivity of the error to the exponential decay exponent shown throughout the article illustrates that even in the event of under or over estimation of the value of the decay exponent, the bias in the error estimation and optimal locations is small, which shows quantitatively that the model is robust for the application illustrated here. And with regard to this, we intend to test the model using multiple other datasets as they become available, using environments with different characteristics to further illustrate the applicability of the model in several conditions. These tests are not

included as part of this article as the length and extend of the article would be much longer than it already is, the main focus of this manuscript is to present the approach in detail in hope that the community builds on its applicability, aside from our own application to other datasets after this presentation.

2) Snow distribution in mountain environments has been shown to be consistent within season and from year to year because the controlling processes are relatively consistent from season to season (Deems et al., 2008; Sturm and Wagner, 2010; Schirmer et al., 2011; Melvold and Skaugen, 2013; Helfrich et al., 2014). For example, predominant wind directions lead to the formation of snow drifts in locations consistent from year to year according to these predominant directions and the relative orientation of topographic features. Similarly, in forested environments, canopy interception is a dominant factor affecting the spatial patterns of distribution of snow (Trujillo et al., 2007; Trujillo et al., 2009), which in the absence of major disturbances, remains a dominant process from season to season, and also within the season. These observations suggest that the correlation/covariance model should also be consistent, as well as the parameters of the model. These parameters can be estimated via a dense survey of one or more small plots of a size similar to that that is aimed to be represented, or via Laser scanning. These surveys would not have to be repeated as the parameters and covariance models should be preserved. We will be working on further illustrating this with further implementation of the method here.

- It was not clear to me why the three-point profile analysis (section 4.2) and the fivepoint two-dimensional analysis (section 5.2) were conducted. These types of manual snow surveys may be somewhat unconventional, as it is more common to have 10 or more measurements made in a single profile. The main example that I can recall that had 3-5 point types of surveys is the CLPX experiment (see Elder et al. 2009), which was a specialized measurement campaign, so I think it is necessary to cite this study (and any other studies with similar snow surveys) in order to clarify the motivation for the analyses in section 4.2 and 5.3. The other two analyses have clear relevance for snow depth stations (one point) and more typical snow surveys (n points), but the other analyses needs more definitive motivation.

RE: Thank you for pointing this out, and we hope to clarify this here. We are including these cases for the following reasons: the two cases with a fixed number of measurements (1D/3-point, 2D/5-point) provide the opportunity to illustrate how the methodology can be used to determine an optimal location on the basis of error minimization. The 3-point example is used to show how an explicit analytic solution can be achieved, and how such analytical solution does indeed correspond to the observations using the case of snow depth. The 5-point example is then an extension of this, although for this 2D case, no explicit analytical solution can be achieved, and the methodology can only be applied numerically. The former case presents a more formal and elegant solution, and the latter presents a more practical solution, and one that will most likely be faced in practice. Also, let us mention that there are indeed a number of examples in the literature that do use these 3-point and 5-point pattern, in some cases without addressing the issue of the representativeness of the measurements (e.g., Molotch, 2009; Jepsen et al., 2012)

- If researchers were planning a snow survey (1-d profile instead of 2-d grid), how might they estimate the exponential decay exponent (v) in order to estimate a_optimal? (page 16) The v values considered here vary by an order of magnitude and are demonstrated to have a substantial impact on the normalized squared error (Fig

10). The authors suggest (page 18, lines 5-7) that LIDAR or dense manual measurements can characterize the covariance/correlation characteristics, but what can be done if resources are unavailable for application of these detailed methods (a realistic scenario that is acknowledged by the authors, page 25, lines 1-3)? If resources are available for LiDAR surveys, then this eliminates the need for manual snow measurements in the first place (and determination of the v parameter), so this issue needs more attention in the text.

RE: *Thank you again as this is indeed an important point. As mentioned above, one issue in favor of the approach is the consistency of the spatial patterns of distribution of snow depth. This implies that because of this consistency, the parameters to characterize the spatial memory do not change as much to require such repeated measurements. For example, a detail survey can be conducted under different conditions to characterize the range of the correlation parameters. With these parameters, not only the parameter that could be used for a particular set of conditions (e.g., after a snow storm, or close to peak accumulation) can be estimated, but also the range in the error and/or optimal locations can be estimated. Another possibility is to perform such surveys (e.g., with TLS) once for several conditions, and characterize the range of possible values for the correlation function parameters. Also here, we should point out that although we show results for a wide range of the exponential decay exponent values, we are finding that most of the values that we have observed are in the lower range of those presented (e.g., 0.1-0.2 m^{-1}). Hence, the biases in the estimated error and the survey design remain small. We would like to find out more about this using more comprehensive dataset including areas with spatial fields repeated throughout a season and multiple seasons. However, this type of testing will require a significant effort and we would not be able to include such results in the extent of just one manuscript.*

 - Why is the error less sensitive to the exponential decay exponent in the two-dimensional case relative to the one-dimensional case (page 23, lines 18-21)? Does this suggest that snow surveys should always be done in a gridded fashion instead of a profile? I think this is a very useful result and so it would be helpful if the authors explained better why this result emerged.

RE: *Thank you. First, let us point out that the number of measurements increases as a function of the square of the number of points along each axis (e.g., 1, 4, 16,...,N^2), which partly explains why the error decreases so rapidly. Beyond a certain number of measurements regularly distributed in the area, the measurements gather enough information such that there is only a very minor gain with adding any new measurements, regardless of the exponent value. Also, the little sensitivity to v comes from the fact that very rapidly, the increase in the number of points is such that much more information about the surrounding area is gathered by the points. As the reviewer points out, this type of stratified sampling is very efficient at reducing the error and capturing information within and area. If the objective is to only represent a profile section, the stratified sampling provides also a rapid decrease in the error with N, although if the profile were to provide information of the surrounding area (not just the line), a profile would not be as representative as a 2D distributed stratified grid. We added a short reference to this in section 5.3.*

- It would be helpful to have more information about the LiDAR data in Section 3. From what is presented in this section, it is unclear what spatial resolution is achieved with the LiDAR (though this is identified in the abstract and later in the text at page

18, line 12) and also there is no discussion of the uncertainty in the LiDAR measurements (e.g., vegetation-induced errors, slope-induced errors, errors in the snow-on vs snow-off scenes, etc.). How does uncertainty in the LiDAR measurements impact the robustness of the analysis?

RE: *We have added some clarification addressing this comment in the Data section (3). Unfortunately, the manual snow surveys during CLPX were performed about two weeks earlier than when the flights were performed and little could be said about the uncertainty of the LIDAR snow depths. However, the dataset has proven to be highly valuable to address some important scientific questions and we believe that despite of this question, it provides us with an extensively used example. Further testing with other datasets will build on the implementation shown here.*

TECHNICAL COMMENTS/CORRECTIONS

- Page 4, Lines 20-21: It sounds redundant to say ". . . use point measurements to represent snow distribution from point measurements". I recommend deleting one of the phrases with "point measurements".

RE: *Thank you. We have eliminated the second one.*

- Page 7, Line 5: Add "a" before "function".

RE: *Corrected.*

- Page 8, Line 23: delete "at" after "represented" ("at" is already included before "which").

RE: *Corrected.*

- Page 9, Line 26: Please clarify what the "x and y" directions represent. Is x east-west, y north-south?

RE: *Yes. We added "(east)" and "(north)" after x and y, respectively.*

- Page 9, Line 29: The phrasing "overestimate in absolute value terms" is somewhat confusing because it no longer directly conveys that the point values tend to have severe underestimation of snow depth for cases of snow depth below the mean value. Consider rephrasing.

RE: *We realize that the wording might be a bit confusing here. Perhaps we can express this better here. Ultimately, let us consider here two snow depth profiles, one with the snow depths at the nominal scale (~1 m), and a second one with a moving average (MA) of the first one with an averaging window equal to the sampling spacing. Ultimately, the variance/standard deviation of the first profile (~1 m) is larger than that of the MA, with a distribution that reflects these differences. The samples from the first profile will reflect a larger variance than that of the samples from the MA profile as they are drawn from these distributions, and this is what is reflected in the figures to which the text refers to here. We have included this clarification in the text in section 4 as suggested.*

- Page 12, Line 5 (Eq 6): I do not think that "C" has been defined. I assumed it is the covariance?

RE: *Thank you, this is correct. The equation has been corrected to "COV".*

- Page 13, Line 11: It should read "shorter" instead of "sorter".

RE: *Corrected.*

- Page 13, Line 27: It should be "consists" instead of "consist".

RE: *Corrected.*

- Page 14, Line 21: It should read "three measurements" (plural) in the subsection title.

RE: *Corrected.*

- Page 15, Line 14: This should either read "as an advantage" or "as advantageous".

RE: *Corrected.*

- Page 16, Line 6: Delete "to" after "estimation of".

RE: *Corrected.*

- Page 17, Line 3: It should read "N measurements" (plural) in the subsection title.

RE: *Corrected.*

- Page 18, Lines 3-4: I recommend adding Sturm and Wagner (2010) to the list of citations here.

RE: *Thank you, we have included the reference.*

- Page 23, Lines 8-10: These results are for the two-dimensional case at RW, but how does the model perform at RW?

RE: *We have focused on the isotropic case for the two-dimensional examples. The reason for this is mainly for simplicity as we present the method in the context of snow depth. We intend to build on this as we extend the developments to the anisotropic cases, which would be required for the case of RW. The snow depth field in FS has been shown to exhibit little directionality and low anisotropy versus the field in RW (Trujillo et al., 2007). This is however an important point by the reviewer, and this analysis will need to complement further application of this method, especially for open environments with strong influence of wind redistribution of snow and/or preferential deposition driven by the interaction with topography.*

TABLE AND FIGURE COMMENTS

- Figure S1 (supplement) – This figure appears to be missing. There are supposed to be three figures in the supplement, but only two are provided.

RE: *We apologize if this is the case. However, in the pdf that we can still download from the website we see the three supplementary figures. Figure S1 illustrates the balance between the different terms of the equation. There may have been a problem with the pdf, in which case we would be happy to provide a new version.*

CITATIONS

Elder, K., Cline, D., Liston, G. E., & Armstrong, R. (2009). NASA Cold Land Processes Experiment (CLPX 2002/03): Field Measurements of Snowpack Properties and Soil Moisture. Journal of Hydrometeorology, 10(1), 320–329. doi:10.1175/2008JHM877.1

Sturm, M., and A. M. Wagner, 2010: Using repeated patterns in snow distribution modeling: An Arctic example. Water Resour. Res., 46, 1–15, doi:10.1029/2010WR009434.

References

Deems, J. S., Fassnacht, S. R., and Elder, K. J.: Interannual Consistency in Fractal Snow Depth Patterns at Two Colorado Mountain Sites, *J. Hydrometeor., 9*(5), 977-988, doi: 10.1175/2008jhm901.1, 2008.

Helfrich, K., Schöber, J., Schneider, K., Sailer, R., and Kuhn, M.: Interannual persistence of the seasonal snow cover in a glacierized catchment, *J. Glaciol., 60*(223), 889-904, doi: 10.3189/2014JoG13J197, 2014.

Jepsen, S. M., Molotch, N. P., Williams, M. W., Rittger, K. E., and Sickman, J. O.: Interannual variability of snowmelt in the Sierra Nevada and Rocky Mountains, United States: Examples from two alpine watersheds, *Water Resour. Res., 48*(2), W02529, 2012.

Melvold, K., and Skaugen, T.: Multiscale spatial variability of lidar-derived and modeled snow depth on Hardangervidda, Norway, *Ann. Glaciol., 54*(62), 273-281, 2013.

Molotch, N. P.: Reconstructing snow water equivalent in the Rio Grande headwaters using remotely sensed snow cover data and a spatially distributed snowmelt model, *Hydrol. Processes, 23*(7), 1076-1089, 2009.

Schirmer, M., Wirz, V., Clifton, A., and Lehning, M.: Persistence in intra-annual snow depth distribution: 1. Measurements and topographic control, *Water Resour. Res., 47*(9), W09516, 2011.

Sturm, M., and Wagner, A. M.: Using repeated patterns in snow distribution modeling: An Arctic example, *Water Resour. Res., 46*, 2010.

Trujillo, E., Ramirez, J. A., and Elder, K. J.: Topographic, meteorologic, and canopy controls on the scaling characteristics of the spatial distribution of snow depth fields, *Water Resour. Res., 43*, W07409, doi: 10.1029/2006WR005317, 2007.

Trujillo, E., Ramírez, J. A., and Elder, K. J.: Scaling properties and spatial organization of snow depth fields in sub-alpine forest and alpine tundra, *Hydrol. Processes, 23*, 1575–1590, doi: 10.1002/hyp.7270, 2009.

THEORETICAL ANALYSIS OF ERRORS WHEN ESTIMATING SNOW DISTRIBUTION THROUGH POINT MEASUREMENTS

By

Ernesto Trujillo[1, 2] and Michael Lehning [2, 1]

1. School of Architecture, Civil and Environmental Engineering, École Polytechnique Fédérale de Lausanne, Lausanne, Switzerland

2. WSL Institute for Snow and Avalanche Research SLF, Davos, Switzerland

Corresponding Author:

Ernesto Trujillo
EPFL ENAC IIE CRYOS, Station 2
Lausanne, Switzerland, CH-1015
Email: Ernesto.Trujillo@epfl.ch
Office: +41 21 693 5938

24   **Abstract**

25   In recent years, marked improvements in our knowledge of the statistical properties of the

26   spatial distribution of snow properties have been achieved thanks to improvements in measuring

27   technologies (e.g., LIDAR, TLS, and GPR). Despite of this, objective and quantitative

28   frameworks for the evaluation of errors and extrapolations in snow measurements have been

29   lacking. Here, we present a theoretical framework for quantitative evaluations of the uncertainty

30   of point measurements of snow depth when used to represent the average depth over a profile

31   section or an area. The error is defined as the expected value of the squared difference between

32   the real mean of the profile/field and the sample mean from a limited number of measurements.

33   The model is tested for one and two dimensional survey designs that range from a single

34   measurement to an increasing number of regularly-spaced measurements. Using high-resolution

35   (~ 1m) LIDAR snow depths at two locations in Colorado, we show that the sample errors follow

36   the theoretical behavior. Furthermore, we show how the determination of the spatial location of

37   the measurements can be reduced to an optimization problem for the case of the predefined

38   number of measurements, or to the designation of an acceptable uncertainty level to determine

39   the total number of regularly-spaced measurements required to achieve such error. On this basis,

40   a series of figures are presented that can be used to aid in the determination of the survey design

41   under the conditions described, and under the assumption of prior knowledge of the spatial

42   covariance/correlation properties. With this methodology, better objective survey designs can be

43   accomplished, tailored to the specific applications for which the measurements are going to be

44   used. The theoretical framework can be extended to other spatially distributed snow variables

45   (e.g., SWE) whose statistical properties are comparable to those of snow depth.

1   Introduction

46

47   The assessment of uncertainties of snow measurements remains a challenging problem in

48   snow sciences. Snow cover properties are highly heterogeneous over space and time and the

49   representativeness of measurements of snow stage variables (e.g., snow depth, snow density, and

50   snow water equivalent (SWE)) is often overlooked due to difficulties associated with the

51   assessment of such uncertainties. This has been, at least in part, due to the limited knowledge of

52   the characteristics of the spatial statistical properties of variables such as snow depth and SWE,

53   particularly at the small-scales (sub-meter to tens of meters). However, a turning point has been

54   reached in recent years thanks to improvements in remote sensing of snow (e.g., light detection

55   and ranging (LiDAR) and Radar technologies), which have allowed significant progress in the

56   quantitative understanding of the small-scale heterogeneity of snow covers in different

57   environments, with resolutions and areas of coverage previously unresolved with the standard

58   methods of measurement (e.g., Trujillo et al., 2007; Trujillo et al., 2009; Mott et al., 2011).

59   Point or local measurements of snow properties will continue to be necessary for purposes

60   that range from inexpensive evaluation of the amount of snow over a particular area, to

61   validation of models and remote sensing measurements. Such measurements have a footprint

62   representative of a very small area surrounding the measurement location (i.e., support,

63   following the nomenclature proposed by Blöschl (1999)), and the integration of several

64   measurements is necessary for a better representation of the snow variable in question over a

65   given area. Because of this, tools for quantitative evaluations of the representativeness and

66   uncertainty of measurements need to be introduced, and the uncertainty of such measurements

67   should be more widely discussed in the field of snow sciences.

68   Currently, efforts to assess the reliability and uncertainty of snow measurements have

69   focused on statistical analyses using point measurements (e.g., Yang and Woo, 1999; Watson et

70   al., 2006; Rice and Bales, 2010; Lopez-Moreno et al., 2011; Meromy et al., 2013) or

71   synthetically generated fields in a Monte Carlo framework (e.g., Kronholm and Birkeland, 2007;

72   Shea and Jamieson, 2010), and comparisons between remotely sensed and ground data (Chang et

73   al., 2005; Grünewald and Lehning, 2014). These studies have been useful to empirically quantify

74   uncertainties associated with point measurements; However, these type of approaches do not

75   provide a quantitative framework for the assessment of uncertainties associated with a particular

76   sampling design, they do not allow for an optimal sampling strategy (e.g., selecting the number

77   of points and locations for a desired accuracy level), and they do not take advantage of the

78   increased knowledge of the characteristics of the heterogeneity of snow cover properties.

79   Another possible approach is one in which the expected error in the estimation of a particular

80   statistical moment of a field over a defined domain (e.g., areal mean or standard deviation from a

81   finite number of measurements) is determined on the basis of known statistical properties of the

82   field in question. Such approach uses geostatistical principles that have been proposed by

83   Matheron (1955; 1970) and others, and that have been applied in mining geostatistics (Journel

84   and Huijbregts, 1978), the analysis of uncertainties when measuring precipitation (Rodríguez-

85   Iturbe and Mejía, 1974), and for a more general analysis of the effects of sampling of random

86   fields as examples of environmental variables (e.g., Skøien and Blöschl, 2006), among others.

87   Despite of these examples, there is to the authors' knowledge no attempt of implementing such

88   type of approach in snow sciences, tailoring the methodology to the particular analysis of

89   uncertainties when measuring snow variables such as snow depth. Such an implementation

90   appears to be lacking in numerous studies that use point measurements to represent snow

Ernesto Trujillo 2/4/2015 11:18
Deleted: design

Ernesto Trujillo 1/4/2015 15:56
Deleted: has been explored for

93 distribution, addressing the spatial extrapolation of such point measurements as the "true" spatial

94 distribution of snow depth when evaluating the performance of interpolation methodologies,

95 regressions trees, and hydrological models. These comparisons ignore the intrinsic error incurred

96 when extrapolating the original point measurements, leaving a proportion of uncertainty that can

97 be significant unaccounted for. This is the principal motivation of the present study, with the

98 intention of spreading the use of more objective and quantitative methodologies for error

99 evaluation in snow sciences. Also, the approach that is presented below can be used for objective

100 survey design to estimate snow distribution from point measurements. We do not intend to

101 present our approach as novel in the general geostatistical sense; instead, we present the

102 derivation with the specific application for snow sciences in mind. However, because of the

103 general nature of the random fields' theory that the development is based on, similar

104 developments can indeed be applied to other environmental variables that can be described as a

105 random field.

106   On this basis, the error in the estimation of spatial means from point measurements over a

107 particular domain (e.g., a profile, or an area) can be quantified as the expected value of the

108 squared difference between the real mean and the sample mean obtained from a limited number

109 of point measurements. Such an approach, as it will be shown here, uses spatial statistical

110 properties of snow depth fields in a way that allows for an objective evaluation of the estimation

111 error for snow depth measurements. The sections below illustrate the use of such methodology

112 for optimal design of sample strategies in the specific context of snow depth. However, the

113 methodology can also be implemented for other snow variables such as snow water equivalent,

114 given that similar geostatistics can be used to characterize their spatial organization.

Ernesto Trujillo 26/3/2015 16:45
Deleted: from point measurements

Ernesto Trujillo 1/4/2015 16:12
Deleted: Additionally,

Ernesto Trujillo 2/4/2015 11:23
Deleted: he development of the expression to evaluate the error presented here includes some additional terms that appear in the derivation of the expression that are not accounted for in developments. These terms are needed to accurately predict the behavior that is observed when measuring snow depth from a limited number of measurements.

2   Background

Let $Z(\mathbf{x})$ denote a random field function of the coordinates $\mathbf{x}$ in the n-dimensional space $\mathbb{R}^n$. Bold letters represent a location vector from hereon. In our case, the field can represent e.g.: snow depth or snow water equivalent (SWE) at a given time of the year. The mean of the process over a domain A (e.g., a profile section or an area) is defined as:

$$\mu_z(A) = \frac{1}{A}\int_A z(\mathbf{x})d\mathbf{x} \qquad (1)$$

In practice, the mean is often obtained from the arithmetic average of measurements at a finite number of locations, N, within the domain:

$$\overline{Z} = \frac{1}{N}\sum_{i=1}^{N} z(\mathbf{x}_i) \qquad (2)$$

The performance of the estimator $\overline{Z}$ can be evaluated by calculating the expected value of the square difference between the estimator $\overline{Z}$ and the true mean $\mu_z(A)$

$$\sigma_{\overline{Z}}^2(A) = E\left[\left(\frac{1}{N}\sum_{i=1}^{N} z(\mathbf{x}_i) - \frac{1}{A}\int_A z(\mathbf{x})d\mathbf{x}\right)^2\right] \qquad (3)$$

For a 1st order stationary process (i.e., the mean independent of location; e.g., Cressie (1993), section 2; and Journel and Huijbregts (1978), section 2), (3) can be expressed as

$$
\begin{aligned}
\sigma_{\overline{Z}}^2(A) = {} & \frac{1}{N^2}\sum_{i=1}^{N} VAR\left[z(\mathbf{x}_i)\right] + \frac{2}{N^2}\sum_{i=1}^{N-1}\sum_{j=i+1}^{N} COV\left[z(\mathbf{x}_i)z(\mathbf{x}_j)\right] \\
& -\frac{2}{N\cdot A}\sum_{i=1}^{N}\int_A COV\left[z(\mathbf{x}_i)z(\mathbf{x}_j)\right]d\mathbf{x}_j \qquad (4)\\
& +\frac{1}{A^2}\int_A\int_A COV\left[z(\mathbf{x}_i)z(\mathbf{x}_j)\right]d\mathbf{x}_i\,d\mathbf{x}_j
\end{aligned}
$$

140   where VAR[ ] and COV[ ] are the variance and the covariance, respectively. If we further

141   assume that the process is second order stationary (e.g., Cressie (1993), section 2; and Journel

142   and Huijbregts (1978), section 2), that is, if the mean and the variance are independent of the

143   location, and the covariance function depends only on the vector difference $\mathbf{x}_i - \mathbf{x}_j$. (3) can be

144   expressed as

145
$$\sigma_{\bar{Z}}^2(A) = \sigma_p^2 \left[\begin{array}{l} \dfrac{1}{N} + \dfrac{2}{N^2} \sum_{i=1}^{N-1} \sum_{j=i+1}^{N} CORR\left[\mathbf{x}_i - \mathbf{x}_j \right] \\ -\dfrac{2}{NA} \sum_{i=1}^{N} \int_A CORR\left[\mathbf{x}_i - \mathbf{x}_j \right] d\mathbf{x}_j \\ +\dfrac{1}{A^2} \int_A \int_A CORR\left[\mathbf{x}_i - \mathbf{x}_j \right] d\mathbf{x}_i \, d\mathbf{x}_j \end{array} \right]$$
(5)

146   where CORR[ ] is the correlation function, and σ_p^2 is the variance of the point process.

147   The first two terms in (5) are the total sum of the covariances (or correlation as σ_p^2 has been

148   factored out) between all point locations $i = 1,\ldots,N$ (e.g., measurement locations). The first of

149   the two terms is only a function of the number of points, while the second is a function of the

150   number of points, N, and the correlations between the locations. Such correlations are themselves

151   a function of the separation vectors (both in magnitude and direction), and the parameters of the

152   correlation function. These two terms are independent of the size of the area A, and can be

153   thought of as the portion of the error caused by the correlation between the point processes at the

154   locations $i = 1,\ldots,N$ (e.g., measurement locations). Term 3 accounts for the correlation between

155   the measurement locations and the continuous process over the domain A. This term can be seen

156   as a negative contribution to the total error assuming that the sum of the integrals is positive. The

157   term is a function of the number of points, N, the domain area, A, the location of the points and

158   the correlation structure, characterized using the parameters of the correlation function. Lastly,

159   term 4 is the contribution to the error caused by the intrinsic correlation structure of the

160   continuous process over the domain. This term is a function of the domain (e.g., size and shape

161   of A) and the correlation structure (e.g., parameters of the correlation function).

3   Data

163   For the analyses and tests of the methodology presented here, Light Detection and Ranging

164   (LIDAR) snow depths obtained as part of the NASA's Cold Land Processes Experiment (CLPX)

165   will be used (Cline et al., 2009). The dataset consists of spatially distributed snow depths for 1-

166   km x 1-km areas (Intensive Study Areas - ISAs) in the Colorado Rocky Mountains close to

167   maximum snow accumulation in April, 2003. The data were processed from snow-on (8-9 April,

168   2013) and snow-off (18-19 September, 2013) LIDAR elevation returns with an average

169   horizontal spacing of 1.5 m and vertical tolerance of 0.05 m. The final CLPX snow depth

170   contour product (0.10 m vertical spacing) was generated from these returns. This product was

171   used to generate gridded snow depth surfaces with 1024x1024 elements over the ISAs, for a grid

172   resolution of 0.977 m. For this study two areas will be used: the Fraser – St Louis Creek ISA

173   (FS) and the Rabbit Ears – Walton Creek ISA (RW) (Figure 1). The FS ISA is covered by a

174   moderate density coniferous (lodgepole pine) forest on a flat aspect with low relief. The RW ISA

175   is characterized by a broad meadow interspersed with small, dense stands of coniferous forest

176   and with low rolling topography. The snow depth distributions in these ISAs show differences

177   that are relevant for the analysis of the methodology introduced here. At the FS ISA, the snow

178   depth distribution is relatively isotropic (Figure 1b), with short spatial correlation memory and

179   little variations in the spatial scaling properties (i.e., power-spectral exponents and scaling

180   breaks) with direction (Trujillo et al., 2007). On the other hand, the spatial distribution of snow

182 depth in the RW ISA is more anisotropic (Figure 1c), with longer spatial correlation memory

183 along a principal direction aligned with the predominant wind direction versus shorter memory

184 along the perpendicular direction, and with variations in the power-spectral exponents and

185 scaling breaks according to the predominant wind directions (Trujillo et al., 2007).

4   One-dimensional process

187   The spatial representation of the snow cover requires a basic assumption on the scale or

188 resolution at which a field or profile is going to be represented. This relies on the spatial support

189 of the measurements. For the case of snow depths, point measurements from local surveys using

190 a snow depth probe are frequently used for this representation. Generally, there are additional

191 sources of uncertainty associated with these types of measurements, such as the accuracy of the

192 position of the measurement in space or deviations in the vertical angle of penetration of the

193 probe through the snow pack. These uncertainties are additional to any of the uncertainties

194 estimated using the methodology discussed here.

195   The one-dimensional case provides a good opportunity to illustrate the limitations of point

196 measurements. Consider the case of a snow depth profile that is measured using a snow depth

197 probe at a regular spacing "d". Each of these point measurements is meant to represent the mean

198 snow depth over a particular distance surrounding the measurement, and the question is: over

199 what distance is such assumption valid? In this case, the intrinsic assumption is that the

200 measurement is representative over the distance "d", but at this point the validity of such

201 assumption is not proven.

202   The answer to this question is conditioned to how variable the profile is and over what

203 distances. To look at this, let us look at two snow depth profiles, one in a forested environment

205   (FS) and another in an open environment (RW) in the Colorado Rocky Mountains (Figure 2a and

206   Figure 3a, respectively). The variability in the profiles is markedly different, with variations over

207   shorter distances in the forested area, and a smoother profile in the open and wind influenced

208   environment. This is reflected in the spatial correlation structure of these snow depth profiles,

209   with stronger correlations over longer distances in open and wind-influenced environments with

210   respect to that in forested environments (Trujillo et al., 2007; Trujillo et al., 2009). These

211   differences should be considered when selecting the sampling frequency required to capture the

212   variability and accurately represent the mean conditions within a particular sampling spacing.

213   This is illustrated by comparing the mean snow depth for a particular resolution to the point

214   value at the center of the interval (Figure 2b in a forested environment and Figure 3b in an open

215   and wind-influenced environment). In the Figures, average versus point values at several

216   sampling intervals are compared for normalized profiles $(\mu = 0, \sigma = 1)$ separated every 30 m in

217   both the x (east) and y (north) directions and for an area of 500 m by 500 m. The 30-m separation

218   between profiles is chosen to reduce the spatial correlation between them. Firstly, the resulting

219   comparison shows that the point values generally overestimate the variability in mean snow

220   depths if we replace the mean snow depth distribution by its point sample. To clarify this, let us

221   consider here two snow depth profiles, one with the snow depths at the nominal scale (~1 m),

222   and a second one with a moving average (MA) of the first one with an averaging window equal

223   to the sampling spacing. Ultimately, the variance/standard deviation of the first profile (~1 m) is

224   larger than that of the MA, with a distribution that reflects these differences. The samples drawn

225   from the first profile will reflect a larger variance than that of the samples from the MA profile as

226   they are drawn from these distributions, and this is what is reflected in Figure 2 and Figure 3.

227   The degree of overestimation can be quantified through the slope of the regression line (in red in

228   Figure 2b and Figure 3b). In the forested environment (Figure 2b), the slopes range between 0.8

229   and 0.13, with decreasing slopes with increasing spacing. These slopes indicate that, on average,

230   the mean values are 0.8 times the point values for the 5 m spacing and 0.1 times the point values

231   for the 100 m spacing. In the open and wind-dominated environment, the slopes are higher and

232   range between 0.97 and 0.23 from 5 m spacing and 100 m spacing, respectively. A clear

233   difference emerges: forested environments require shorter separation between single

234   measurements if the snow depth profile is to be accurately captured by the measurements. The

235   variability within the size of the interval determines the degree of uncertainty associated with the

236   point measurements, as the sub-interval variability is related to the degree of overestimation of

237   the mean value within the interval. Secondly, the differences between average and point values

238   for each spacing distance are generally more scattered in the forested environment than in the

239   open environment, and in both environments the degree of scattering increases with spacing

240   (Figure 2c and Figure 3c). However, it is important to note here that we are comparing

241   normalized profiles ($\mu = 0$, $\sigma = 1$), allowing us to focus on the rescaled spatial variations. What is

242   highlighted is the relevance of the spatial structure of the profile rather than the absolute

243   variance. This spatial structure can be quantified by, for example, the spatial

244   covariance/correlation function.

245   Additionally to the differences in the correlation structure, there are also differences in the

246   absolute variability in snow depth in these environments (Figure 4). As opposed to the

247   normalized snow depth discussed above, the subinterval standard deviation as a function of

248   interval size along the profiles is higher in the open and wind-influenced environment at RW

249   versus the forested environment at FS (Figure 4a). Mean standard deviation values in the open

250   environment are twice as large as those at the forested environment towards the larger interval

253   sizes (~100 m). The standard deviation increases with interval size in both environments, with

254   the steepest increase at the lower interval sizes. Furthermore, the standard deviation tends to

255   stabilize more rapidly in the forested environments, with an increase of only 1.8 cm between 30

256   m and 100 m. On the other hand, the standard deviation continues to increase in the open

257   environment at RW, with less of an asymptotical behavior for the scales analyzed.

258   Complementary, the shaded areas (25% to 75% quantiles) give an idea of the variability of

259   standard deviation values, with a much wider range in RW versus FS, and an increase in the

260   range between quantiles with interval size in RW.

261   Consistent with the standard deviation, the sub-interval mean range (range defined as the

262   difference between the maximum and minimum snow depths within an interval) increases with

263   interval size in both FS and RW (Figure 4b). However, the mean range is larger in the open

264   environment at RW and the rate of increase with interval size is also steeper. Similarly, the

265   shaded areas indicate wider distribution of range values in the open environment at RW, while

266   relatively uniformly distributed around the mean across interval sizes in the forested environment

267   at FS. The results in Figure 2-Figure 4 illustrate this contrasting behavior between the snow

268   covers in these environments and their influence on measurement strategies: that is, the forested

269   environments requires shorter separation between measurements for accurate representation of

270   the snow cover, however, in the wind-influence and open environment, the subinterval

271   variability is higher indicating wider variations around any sampled measurement within the

272   interval.

273   Ultimately, the number and distance between measurements and the specific arrangement of

274   the measurements are all conditioned to what the measurements are needed for. Hydrologic

275   applications may not require a highly detail representation of a snow depth profile (or a field),

Ernesto Trujillo 2/4/2015 11:27
Deleted: in within

Ernesto Trujillo 2/4/2015 11:27
Deleted: The

Ernesto Trujillo 2/4/2015 11:28
Deleted: Also important

Ernesto Trujillo 2/4/2015 11:29
Deleted: two compensating

Ernesto Trujillo 2/4/2015 11:29
Deleted: differences

281   and representing the average conditions over a given distance (or area) is sufficient, but small-

282   scale process-based studies may require a more detailed characterization over shorter distances

283   (or smaller areas). This implies that the decision depends on the particular use that the

284   measurements will support. In the following sections, the equations presented in the Background

285   (section 2) will be applied to evaluate the uncertainty associated with multiple measurement

286   designs for profiles and fields of snow depth.

287 **4.1   Case 1: Single measurement along a profile section**

288   Equation (2) can be used to evaluate the uncertainty of a single measurement along a profile

289   section of length L. For this case, as well as for the following cases in this article, an exponential

290   covariance with a decay exponent v ($v > 0$) will be assumed:

291 $$COV(\mathbf{h},\sigma,v) = \sigma^2 \exp(-v\|\mathbf{h}\|) \quad \text{for } \sigma^2 > 0, \text{ and } v > 0 \qquad (6)$$

292   were σ^2 is the variance, and $\|\mathbf{h}\|$ is the length of the vector $\mathbf{h}$. For this one-dimensional case

293   and combining (6) and (5), the following expression is obtained:

294 $$\sigma_{\bar{Z}}^2(x,L,v)\big/\sigma_p^2 = 1 - \frac{2}{Lv}\left[2 - \exp(-vx) - \exp(-v \cdot [L-x])\right] + \frac{1}{L^2 v}\left[2L + \frac{2}{v}\exp(-vL) - \frac{2}{v}\right]$$

295   (7)

296   where x is the distance from one extreme of the section to the location of the measurement

297   (Figure 5a). The normalized squared error $\sigma_{\bar{Z}}^2(x,L,v)\big/\sigma_p^2$ is minimized at x equal to half of the

298   section length, $L/2$, regardless of v. The existence of a correlation in the profile leads to this

299   solution, as the middle location contains more information about its surroundings. Also, this

300   solution is different from the solution for an uncorrelated profile (e.g., white noise), for which

304   the squared error would be equal to the variance, independent of the location of the

305   measurement.

306   The results here are confirmed with an analysis of LIDAR snow depths profiles in FS and

307   RW (Figure 6). The analysis consists of calculating the difference between the mean and the

308   point value for sections of a given length (varied between 10 m – 50 m) and for x (Figure 5a)

309   between 0 and L along the profile sections. Each sample section of length L will provide a single

310   difference for each of the x values. These sample differences are then used to calculate the mean

311   normalized squared error for each x, and the same is repeated for each section length L. The

312   results indicate that the real snow depth profiles behave as predicted by the model of the error,

313   with a minimum error at x equal to half of the section length. Another difference highlighted by

314   these results is the difference between the sample errors in the forested environment (FS) versus

315   the open environment (RW) for the larger interval sizes (e.g., 50 m). The sampled normalized

316   squared error in the forested environment shows only a mild decrease in the square error to

317   around 0.7-0.8 towards the inside of the section length. However, this decrease is achieved for

318   the measurement along most of the interval length with the exception of the extremes. This can

319   be explained by the relationship between the spatial memory of snow depth (e.g., the correlation

320   function) and the section length. Densely forested environments exhibit correlation lengths that

321   are shorter than those in open and wind influenced environments (e.g., Trujillo et al., 2007;

322   Trujillo et al., 2009). As the section length increases beyond such correlation lengths, a

323   measurement location towards the middle of the interval contains less information of the

324   surrounding snow depths in a forested environment (e.g., FS) versus an open and wind

325   influenced environment (e.g., RW). This is observed in Figure 6c versus Figure 6f, with the

326   results in RW showing a more clear minimum towards the center of the profile section. The

330   results also show a poorer performance of the model in RW versus FS, as the exponential

331   correlation model has a poorer fit in RW at the shorter-lag range; However, model performance

332   is improved for longer section lengths (e.g., Figure 6c and f)

333   Model and sampled results thus support that the measurement location can be fixed in the

334   middle of the interval, and the normalized squared error can then be described as a function of

335   both, the exponential decay exponent, v, and the length of the section, L (Figure 7a). The

336   normalized squared error increases with interval length, with a steeper increase for larger

337   exponential decay exponents, for which the squared error approaches that of an uncorrelated

338   field more rapidly. The theoretical model is tested on the snow depth fields at FS and RW. The

339   test consists of calculating the sampled normalized squared error as the average of all squared-

340   differences between the mid-section snow depth and the mean from all LIDAR grid-points

341   within each interval of length L. This is done for profiles separated every 30 m, similar to the

342   analysis above, and for profiles along the x and y directions. The theoretical normalized squared

343   error is estimated from (7) using the exponential decay exponent from the model fitted to the

344   sampled correlation function. The results show that the theoretical model reproduces the sampled

345   squared error remarkably well, even reproducing the anisotropic properties of the correlograms,

346   represented by the different exponents of the exponential model along x and y directions (Figure

347   7b and c). The model also reproduces the different behavior of the squared error between both

348   fields (i.e., FS and RW), showing that the normalized squared error increases more rapidly and is

349   larger in the forested environment (Figure 7b) versus the open environment (Figure 7c).

350   However, it should be noted here that as the error is normalized and as the variance of the field in

351   the open environment is larger (Figure 4a), the absolute squared error could reach higher values

352   in the open environment (RW). In this regard, one feature to discuss here is the assumption that

359   the point variance of snow depth in these environments has been estimated as the spatial variance

360   over the entire study area, as it is generally practiced in time series analysis and geostatistics. In

361   practice, this is the only possible approach because there is limited information to estimate the

362   point variance from multiple realizations of the process at each spatial location, as inter- and

363   intra- annual snow depth fields are not available, not only for these areas, but for almost any area

364   where this methodology may be applied.

365   **4.2   Case 2: Three measurements along a profile section**

366   From (5) it is also evident that increasing the number of measurements will reduce the

367   squared error. In the case of three measurements separated by a distance 'a', with the middle

368   measurement centered in the section of length L (Figure 5b), and for an exponential covariance

369   function with parameter v, (5) leads to the following expression for this particular case:

370
$$\sigma_{\tilde{z}}^2(a,L,v)\big/\sigma_p^2 = \frac{1}{3} + \frac{2}{9}\Big[2\exp(-va) - \exp(-2va)\Big]$$
$$-\frac{4}{3Lv}\left[3 - \exp\left(-\frac{vL}{2}\right)\big(1 + \exp(-va) + \exp(va)\big)\right]$$
$$+\frac{1}{L^2v}\left[2L + \frac{2}{v}\exp(-vL) - \frac{2}{v}\right]$$
(8)

371   Equation (8) can be minimized to determine the optimal separation distance between points,

372   a, as a function of L and v:

373
$$a_{optimal} = -\frac{1}{v}\ln(t)$$
(9)

374   where

375
$$t = \frac{B + \sqrt{B^2 - 4AB}}{2A}$$

377
$$A = \frac{4v}{9}$$

378
$$\text{and } B = -\frac{4}{3L}\exp\left(-\frac{vL}{2}\right)$$

379   The combination of (8) and (9) can be used to determine the normalized squared error,

380   σ_Z^2 / σ_p^2, and the optimal distance, $a_{optimal}$, for the measurement pattern in Figure 5b. The model

381   predicts that the normalized squared error is minimized at an intermediate location between 0

382   and $L/2$ (black lines in Figure 8a and b). The results show an increase in the error with interval

383   size, L, as well as little sensitivity of $a_{optimal}$ to v. This latter feature can be seen as an advantage

384   since small biases in the estimation of v will not result in significant biases in the estimation of

385    $a_{optimal}$. One could almost assume a value of $a_{optimal}$ without prior knowledge of the exponential

386   decay exponent, selecting $a_{optimal}$ within the range of values indicated by the model for a rage of

387   possible exponential decay exponents. Note that $a_{optimal}$ is located close to the 60% distance from

388   the center towards the outer boundary of the profile section for all section lengths (Figure 8a and

389   b). On the other hand, the measurement error displays a higher sensitivity to v around $a_{optimal}$,

390   indicating that biases in the estimation of y would have a more noticeable effect on the

391   estimation of the measurement error. This is further clarified in Figure 8c, in which the

392   normalized error (not squared) and $a_{optimal}$ can be obtained for corresponding profile section

393   lengths (L) and exponential decay exponents (v) based on the isolines shown. For example, for a

394   profile section of 30 m, and an exponential decay exponent of 0.2 m^{-1}, the normalized error is

395   0.32 and $a_{optimal}$ is 9.63 m (see intersect of the two isolines in Figure 8c). The normalized error in

396   Figure 8c is not squared, highlighting the sensitivity of the measurement error to v, which

400 represents the degree of spatial correlation of the profile in this case (e.g., lower values indicate

401 stronger spatial memory/correlation, hence lower measurement errors).

402   The performance of the model is tested against the normalized squared error obtained from

403 the same snow depth profiles in FS and RW. The test consists of estimating the normalized

404 squared error for profiles sections of length between 10 m and 80 m, with a being varied between

405 0 and $L/2$ (Figure 9). For each value of a, the normalized squared error is estimated based on the

406 means obtained using the three snow depth samples for each section. All squared differences are

407 then averaged to obtain the values presented in the Figure. Sampled and modeled errors follow

408 the same trend across all a values and for the different L values in Figure 9. The minimum error

409 is also reproduced by the model proving the applicability of the model for estimating the optimal

410 separation between measurements. The model does perform better in the forested environment of

411 FS versus RW, particularly for lower a values. This can be justified as the exponential

412 covariance model displays a better fit in FS over RW, particularly over the lower range of lag

413 values. Also, note that both the modeled and sampled normalized squared errors are lower for the

414 snow depth profiles at RW because of the longer spatial memory of the snow depth distribution

415 in this environment (higher spatial correlations) when compared to that in FS.

416 **4.3   Case 3: *N* measurements along a profile section**

417   As stated above, the measurement error can be reduced by increasing the number of

418 measurements taken over a given section of length L. Let us focus on the case of stratified

419 sampling where N regularly spaced measurements are taken over the interval (Figure 5c), and to

420 quantify this reduction we can use (5) and the exponential covariance model. Equation (5) can

421 then be reduced to:

$$\sigma_{\bar{Z}}^2(N,L,\nu)/\sigma_p^2 = \frac{1}{N} + \frac{2}{N^2}\sum_{k=1}^{N-1} k\exp\left(-\nu\left[L - \frac{kL}{N}\right]\right)$$

$$- \frac{4}{L\nu}\left[1 - \frac{1}{N}\sum_{k=1}^{N}\exp\left(-\nu\frac{L}{N}\left[N - k + \frac{1}{2}\right]\right)\right] \qquad (10)$$

$$- \frac{2}{L^2\nu^2}\left[1 - L\nu - \exp(-\nu L)\right]$$

The normalized squared error ($\sigma_{\bar{Z}}^2 / \sigma_p^2$) obtained with (10) for profiles sections of lengths between 10 and 80 shows a steep decrease with N (Figure 10), with a steeper decrease for higher exponential decay exponents. For the longer profile sections (e.g., 80, Figure 10d), little reductions are achieved in the squared error beyond only a few measurements (e.g., $N = 16$). Equation (10) and the results in Figure 10 can be used to determine the number of measurements necessary to achieve a desired accuracy level. One could, for example, design a survey to sample a snow depth profile with a mean value every 10 m. The number of measurements required to achieve a desired level of accuracy can be obtained from Figure 10a, based on previous knowledge of the sample estimate of the exponential decay exponent. This can be achieved thanks to the intra-annual and inter-annual persistence of the spatial patterns, and hence, the spatial statistical properties of snow depth fields in mountain environments, as shown in previous studies using both manual surveys and LIDAR measurements (e.g., Deems et al., 2008; Sturm and Wagner, 2010; Schirmer et al., 2011; Melvold and Skaugen, 2013; Helfrich et al., 2014). A detailed spatial survey (e.g., dense manual measurements or TLS), sampling different portions of an area can be used to determine the covariance/correlation characteristics of the snow depth distribution, with which the model for the error can be applied. An a priori estimate of the exponential decay exponent may also be possible and will be tested in future applications of the framework, given the relative insensitivity of the error with respect to ν.

443   Following the method described in the previous section, we test the performance of the

444   model against the normalized squared error obtained from the same snow depth profiles in FS

445   and RW. In this case, the sampled squared error is estimated based on the N regularly-spaced

446   measurements distributed along the profile sections of length L. As the snow depth fields are

447   gridded at ~1-m resolution, the location of the measurements is approximated to the closest

448   coordinate in the profile section following the pattern in Figure 5c. Once again, sampled and

449   modeled errors follow closely the same trend for the different L values in both FS and RW

450   (Figure 11). The error decreases with N, with a rapid decay at the lower N values, illustrating that

451   the error can be drastically reduced by simply increasing the number of measurements by a small

452   amount. The normalized squared error across all N values is lower for RW than for FS,

453   consistent with the higher spatial correlations observed in the snow depth fields of RW versus

454   FS. Once again, there are some differences between the sampled and modeled normalized

455   squared error in RW for the shorter profile lengths and for small N values: a consequence of the

456   poorer fit of the exponential model for the shorter lag range in RW. However, the model is still

457   able to reproduce the error in both fields, and the applicability of the model is illustrated even

458   when the fit of the correlation model can be improved.

459   **5   Two-dimensional process**

460   Similar to the one-dimensional process, equation (5) can be formulated to calculate the

461   squared error in the two-dimensional space. To exemplify this, we apply the methodology to an

462   isotropic process over the x-y plane for three cases in a square area: (a) one single measurement

463   in the center of the area, (b) five measurements radiating out from the center (Figure 12a), and

464   (c) N by N measurements regularly spaced in the x and y directions (Figure 12b).

465   For the isotropic case, the covariance/correlation function is only dependent on the

466   magnitude of the lag vector,

$$h_{i,j} = \left| \mathbf{x}_i - \mathbf{x}_j \right| \qquad (11)$$

467

468

469   and, consequently, the error is represented by,

$$\sigma_{\bar{Z}}^2(A) = \sigma_p^2 \left[\begin{array}{c} \dfrac{1}{N} + \dfrac{2}{N^2} \sum_{i=1}^{N-1} \sum_{j=i+1}^{N} CORR\left[h_{i,j}\right] \\ -\dfrac{2}{NA} \sum_{i=1}^{N} \int_A CORR\left[h_{i,j}\right] d\mathbf{x}_j \\ +\dfrac{1}{A^2} \int_A \int_A CORR\left[h_{i,j}\right] d\mathbf{x}_i\, d\mathbf{x}_j \end{array} \right] \qquad (12)$$

470

471

472   The exponential correlation function for the isotropic case takes the following form:

$$CORR(h,v) = \exp(-vh) \qquad (13)$$

473

474   where h is the magnitude of the lag vector. Replacing into the expression for $\sigma_{\bar{Z}}^2$, we obtain,

$$\sigma_{\bar{Z}}^2 = \sigma_p^2 \left[\begin{array}{c} \dfrac{1}{N} + \dfrac{2}{N^2} \sum_{i=1}^{N-1} \sum_{j=i+1}^{N} \exp\left(-v\left|\mathbf{x}_i - \mathbf{x}_j\right|\right) \\ -\dfrac{2}{NA} \sum_{i=1}^{N} \int_A \exp\left(-v\left|\mathbf{x}_i - \mathbf{x}_j\right|\right) d\mathbf{x}_j \\ +\dfrac{1}{A^2} \int_A \int_A \exp\left(-v\left|\mathbf{x}_i - \mathbf{x}_j\right|\right) d\mathbf{x}_j\, d\mathbf{x}_i \end{array} \right] \qquad (14)$$

475

476   For the case of a rectangular area of side dimension L_x and L_y in the corresponding x and y

477   directions, the equation becomes,

478
$$\sigma_{\overline{Z}}^2 = \sigma_P^2 \left[\begin{array}{l} \dfrac{1}{N} + \dfrac{2}{N^2} \sum_{i=1}^{N-1} \sum_{j=i+1}^{N} \exp\left(-v\left(\left(x_i - x_j\right)^2 + \left(y_i - y_j\right)^2\right)^{1/2}\right) \\ -\dfrac{2}{NA} \sum_{i=1}^{N} \int_0^{L_y} \int_0^{L_x} \exp\left(-v\left(\left(x_i - x\right)^2 + \left(y_i - y\right)^2\right)^{1/2}\right) dx\,dy \\ +\dfrac{1}{A^2} \int_0^{L_y} \int_0^{L_x} \int_0^{L_y} \int_0^{L_x} \exp\left(-v\left(\left(x'-x\right)^2 + \left(y'-y\right)^2\right)^{1/2}\right) dx\,dy\,dx'\,dy' \end{array} \right]$$
(15)

479   The limits of the integrals can be changed depending on the desired location of the origin. In

480 this case, the origin is located at the lower-left corner.

481   As discussed earlier, the first term is only a function of N, such that the base error is the

482 variance of the point process divided by the number of points. The second term is a function of

483 N, the location of the points, and the decay rate v. The third term is a function of N, A, the

484 location of the points, and the decay rate v. The fourth term is a function of A and v, but is

485 independent of the location of the points and N (i.e., independent of the survey design, and only a

486 function of the correlation structure of the continuous process).

487 **5.1   Case 1: Single measurement in the center of the area**

488   In this case, we focus on a single measurement in the middle of a square area of side

489 dimension L. Numerical solution of (15) shows that the normalized squared error increases

490 rapidly with L, with a steeper increase for higher exponential decay exponents (Figure 13a),

491 which approach a normalized squared error of 1 for L values less than 10 (e.g., $1 \le v \le 5$). The

492 theoretical results in Figure 13a can be used to determine the discrepancy between a single

493 measurement in the middle of an area and the areal mean for a second order stationary and

494 anisotropic process with an exponential covariance/correlation function. Comparison of the

495 modeled and sampled normalized square errors for the FS snow depth field indicate very good

496 agreement between modeled and sample errors (Figure 13b). The sample error is estimated

498   following the same procedure explained for the one-dimensional cases, although in the two-

499   dimensional space. Both sampled and modeled errors show the same behavior across L values

500   between 1 m and 100 m, although the scatter in the sampled error increases for larger L values.

501   This can be explained by the smaller number of samples to estimate the mean normalized

502   squared error and the fact that the correlation structure decays rapidly and a single sample

503   becomes less correlated to the surrounding area for these larger areas. The model introduced here

504   can then be used to assess the representativeness of a single measurement over an area

505   objectively and accurately, and it can be extended for other covariance/correlation functions as

506   needed.

507   **5.2   Case 2: Five measurements radiating out from the center of the area**

508   The case five measurements radiating out from the center (Figure 12a), with a point in the

509   middle of the area and four points separated by a distance a from the center leads to a similar

510   optimization problem as illustrated in case 2 of the one-dimensional examples (section 4.2). In

511   the two-dimensional case, (15) does not have an explicit solution for a, and numerical

512   implementation is required. The equation can be solved by simply replacing the point

513   coordinates and the correlation function parameters. Following this approach, the normalized

514   squared error can be obtained for areas of varying sizes (Figure 14). Similar to the one-

515   dimensional example (case 2, section 4.2), $\sigma_{\bar{Z}}^2 \big/ \sigma_p^2$ decreases with a, reaching a minimum at an

516   intermediate distance from the middle point outwards. The decay in $\sigma_{\bar{Z}}^2 \big/ \sigma_p^2$ is more rapid for the

517   least correlated processes (i.e., higher decay exponents) reaching a value close to the base

518   normalized square error that is a function of the number of points (i.e., $1/N = 1/5$ in this case). An

519   extended analysis of the effect of each of the terms in the equation is included in the

Supplementary Information. The error, as shown in Figure 14, is minimized as a consequence of two balancing terms that lead to this intermediate solution. The optimal solution is a balance between reducing the correlation between the individual measurements (e.g., increasing the separation between the location of the measurements) but increasing the correlation between the measurements and the surrounding area (e.g., locating the measurements closer to the middle of the area). These two competing effects lead to an optimization problem based on the location of the point measurements. For the least correlated processes, the error behaves closer to the behavior of an uncorrelated field once the measurements become effectively decorrelated (e.g., a > 1 in Figure 14b for $v = 5$). Figure 14 exemplifies how (15) can be used to determine the optimal measurement location for areas of different sizes, and to determine the associated error with configurations other than the optimal.

The performance of the model is tested against the normalized squared error obtained from the snow depth field in FS. The test consists of estimating the normalized squared error for square areas of side dimension (L) between 10 m and 79 m, with a being varied between 0 and $L/2$ (Figure 15). For each value of a, the normalized squared error is estimated based on the means obtained using the five snow depth samples for each section. All squared differences are then averaged to obtain the values presented in the figure. Once again, the sampled and modeled errors follow the same trend across all a values and for the different L values. The minimum error and $a_{optimal}$ are also reproduced closely by the model, and as the area size increases, the sampled and modeled error approach the error for an uncorrelated field at larger separations (i.e., 0.2). These results illustrate that the performance of the model in the two-dimensional space is remarkable, similar to what was observed in the one-dimensional case.

5.3 Case 3: N by N measurements regularly spaced in the x and y directions

546

547   Similarly to the one-dimensional case, the two-dimensional case of N by N regularly spaced

548 measurements (Figure 12b) leads to a decreasing normalized squared error with N (Figure 16).

549 There is a sharp decrease in the error with just increasing the number of measurements in the

550 lower range of N. The analysis illustrates that stratified sampling, as the one shown here, is an

551 excellent approach to minimizing the error. For example, for the area of 10 by 10, increasing N

552 to 4 ($N^2 = 16$) reduces the normalized squared error to less than 0.05. It is also worth noting here

553 that for this two-dimensional case, the error is less sensitive to the value of the exponential decay

554 exponent (v) for the higher N values as the mean is accurately captured regardless of the

555 correlation of the field. Beyond a certain number of measurements regularly distributed in the

556 area, the measurements gather enough information such that there are only very minor

557 improvements with the addition of new measurements, regardless of the exponent value. Figure

558 16 serves as an example of how the methodology can be used for objective selection of the

559 number of measurements necessary to achieve a desired accuracy level using prior knowledge of

560 the spatial covariance function.

561   The performance of the model is tested again for square areas of side dimension (L) between

562 10 m and 79 m using the snow depth field in FS, and for an increasing number of rows/columns

563 of measurements leading to a total number of measurements of N^2 (Figure 17). The results

564 illustrate again the accurate performance of the theoretical model, with sampled and model errors

565 following closely the same squared errors. Both sampled and modeled errors increase as the size

566 of the area increases, as expected. These results complete the model performance tests for the

567 two-dimensional isotropic case.

6 Summary and Conclusions

A methodology for an objective evaluation of the error in capturing mean snow depths from point measurements is presented based on the expected value of the squared difference between the real average snow depth and the mean of a finite number of snow depth samples within a defined domain (e.g., a profile section or an area). The model can be used for assisting the design of survey strategies such that the error is minimized in the case of a limited and predetermined number of measurements, or such that the desired number of measurements is determined based on a predefined acceptable uncertainty level. The model is applied to one- and two-dimensional survey examples using LIDAR snow depths collected in the Colorado Rockies. The results confirm that the model is capable of reproducing the estimation error of the mean from a finite number of samples for real snow depth fields.

Here, we should highlight some of the implications of the assumptions made in the model. In simplified terms, the second-order stationarity assumption implies that the mean and the variance of the process/variable (e.g., snow depth) are independent of the spatial location, and that the covariance is dependent only on the separation vector (i.e., lag). Although these assumptions may not be as adequate over larger scales (e.g., greater than 100 m), at smaller scales the assumption in the context of the model application to snow depth should be valid. We present these examples to show how the error can be quantified with good accuracy around such smaller scales. Application of such types of approaches at larger scales will require additional evaluations with particular attention as to what the specific demands of the application are. Also, the methodology as presented here is not suitable for discontinuous snow covers if both snow-covered and snow-free areas are considered in the error estimation. This case has not been considered in the development here.

591   Implementation of the model in practice requires prior assumption of a

592 correlation/covariance model and estimates of the parameters of this model (e.g., the decay

593 exponent for the exponential case). In the examples here we use LIDAR data for the parameter

594 estimation, which we have done to illustrate the applicability of the model and its ability to

595 estimate the error using real snow depth data. Snow distribution in mountain environments has

596 been shown to be consistent intra- and inter-annually because the controlling processes are

597 relatively consistent during the season and from season to season. Such consistency suggests that

598 the correlation/covariance model should also be consistent, as well as the parameters of the

599 model. These parameters can be estimated via a dense survey either manually or with TLS of one

600 or more small plots of a size similar to the size that is aimed to be represented. These surveys

601 would not necessarily have to be repeated as the parameters and covariance models should be

602 preserved. Detailed surveys can be conducted under different conditions to characterize the range

603 of the correlation models and parameters (e.g., after a snow storm, or close to peak

604 accumulation). Also here, we should point out that although we show results for a wide range of

605 the exponential decay exponent values, we are finding that most of the values that we have

606 observed are in the lower range of those presented (e.g., 0.1-0.2 m^{-1}). Hence, the biases in the

607 estimated error and the survey design remain small.

608   Currently, remote sensing technologies (e.g., TLS, Airborne LiDAR, and ground penetrating

609 radar) are allowing for the characterization of snow cover properties at increasing resolutions in

610 both space and time. Such improvements can be utilized in the context presented here providing

611 information about the range of best fitting covariance/correlation models and parameters for

612 different conditions, supporting the application of methodologies such as the one presented here.

613 With such improvements, survey designs can be optimized such that estimation errors can be

626   explicitly addressed and accounted for, particularly when extrapolating a limited number of

627   measurements to estimate the spatial distribution of snow. Such applications will continue to be

628   relevant despite of the aforementioned improvements, as access to these technologies is limited

629   by their cost and the expertise that is required for their application.

630
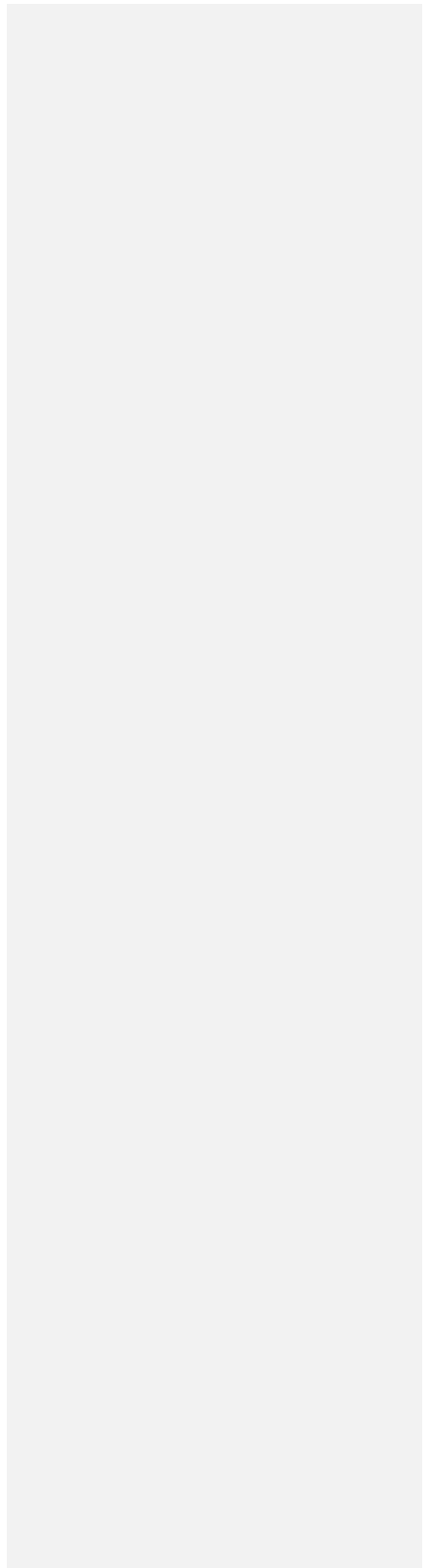
631

7   Acknowledgements

635

636

Figures

638   Figure 1. (a) Location of the Fraser and Rabbit Ears study areas in the state of Colorado (in
639   grey). (b) LIDAR Snow depth distributions on April 8, 2003, at the Saint Louis Creek Intensive
640   Study Area (ISA) and (c) on April 9 at the Rabbit Ears ISA.

641   Figure 2. (a) Sample normalized snow depth profile (mean = 0, standard deviation = 1) in a
642   forested environment from LIDAR (1-m resolution) at the Fraser – St. Louis Creek (FS)
643   intensive study area (ISA) of the Cold Land Processes eXperiment (CLPX) (Trujillo et al., 2007;
644   Cline et al., 2009). The profile is sampled with regular separations (spacing) of 5 m, 10 m, 25 m,
645   50 m, and 100 m (from top to bottom, respectively). (b) Average values within sampling
646   intervals (same as in (a)) versus point samples for normalized snow depth profiles in the FS ISA.
647   The red line is a linear regression fit, with slope β and r^2 as indicated in each plot. (c) Histograms
648   of the difference between the point and average values for each of the sampling intervals. The
649   vertical red line marks the mean difference.

650   Figure 3. (a) As Figure 2 but for an open and wind influenced environment at the Rabbit Ears
651   – Walton Creek (RW) ISA of the CLPX (Trujillo et al., 2007; Cline et al., 2009). (b) Average
652   values within sampling intervals (same as in (a)) versus point samples for normalized snow depth
653   profiles in the RW ISA. The red line is a linear regression fit, with slope β and r^2 as indicated in
654   each plot. (c) Histograms of the difference between the point and average values for each of the
655   sampling intervals. The vertical red line marks the mean difference.

656   Figure 4. Sub-interval standard deviation (a) and range (b) for varying interval lengths for
657   profiles of snow depth in a forested environment (FS) and an open and wind-influenced
658   environment (RW) in the Colorado Rocky Mountains (same regions as those in Figure 2 and
659   Figure 3). The mean standard deviation and mean range for the study areas are shown by the
660   solid lines, while the shaded areas cover the quantiles between 25% and 75% of the values for all
661   the intervals in these areas.

662   Figure 5. Survey designs for the sampling of a snow profile.

663   Figure 6. Comparison of the theoretical and sampled normalized squared error ($\sigma_{\bar{Z}}^2 / \sigma_p^2$) for
664   the case of a single measurement along a profile section of length L, as in Figure 5a. The survey
665   case applied to profiles in FS and RW along the x and y directions. Solid lines are the theoretical
666   error using exponential decay exponents derived from the functions fitted to the sampled
667   correlation functions of the two surfaces in the x and y directions.

668   Figure 7. (a) Theoretical normalized squared error for a single measurement in the middle of a
669   section of length, L, and for an exponential correlation function with a decay exponent, v. (b) and
670   (c) Comparison of the theoretical and sampled normalized squared error for the same survey case
671   applied to profiles in FS and RW along the x and y directions. Dashed lines are the theoretical
672   error from (7) using exponential decay exponents derived from the functions fitted to the
673   sampled correlation functions of the two surfaces in the x and y directions.

674   Figure 8. (a) and (b) Theoretical normalized squared error for the three-point pattern along a
675   profile section in Figure 5b, and for profile section lengths (L) of 1 (a) and 25 (b). Each of the

Ernesto Trujillo 1/4/2015 18:18
Deleted: dominated

677   colored lines corresponds to a specific decay exponent, ν, and the black line marks the
678   theoretical solution for $a_{optimal}$. (c) Theoretical normalized error and $a_{optimal}$ for isolines of profile
679   section lengths (L) and exponential decay exponents (ν) for the three-point pattern along a profile
680   section of length L in Figure 5b.

681   Figure 9. Theoretical and sampled normalized squared error ($\sigma_{\bar{Z}}^2/\sigma_p^2$) for the three-point
682   pattern along a profile section in Figure 5b, and for profile section lengths (L) between 10 m and
683   80 m in FS and RW. The solid lines are the theoretical error from (8) using exponential decay
684   exponents derived from the functions fitted to the sampled correlation functions of the two
685   surfaces in the x and y directions, while the dots correspond to the sampled error for profiles in
686   FS (a-d) and RW (e-h).

687   Figure 10. Theoretical normalized squared error ($\sigma_{\bar{Z}}^2/\sigma_p^2$) for the N-point pattern along a
688   profile section in Figure 5c, and for profile section lengths (L) between 10 and 80 obtained from
689   (10).

690   Figure 11. Theoretical and sampled normalized squared error ($\sigma_{\bar{Z}}^2/\sigma_p^2$) for the N-point pattern
691   along a profile section in Figure 5c, and for profile section lengths (L) between 10 m and 80 m in
692   FS and RW. The solid point markers are the theoretical error from (10) using exponential decay
693   exponents derived from the functions fitted to the sampled correlograms of the two surfaces in
694   the x and y directions, while the circle markers with the dotted lines correspond to the sampled
695   error for profiles in FS (a-d) and RW (e-h).

696   Figure 12. Sample survey designs with (a) a 5-point pattern centered in the area, and (b) a
697   regularly spaced pattern. For the 5-point pattern, a can vary between 0 and $L/2$, while for the N x
698   N points pattern, the separation between the measurements is determined by the number of
699   points.

700   Figure 13. (a) Theoretical normalized squared error ($\sigma_{\bar{Z}}^2/\sigma_p^2$) for the two-dimensional case
701   with a single measurement in the middle of a square area with side dimension L. (b) Theoretical
702   and sampled normalized squared error for the same two-dimensional survey applied to the snow
703   depth field in FS. The dashed line is the theoretical error derived for an exponential decay
704   exponent of 0.17 derived from the sampled correlation function of snow depth in FS, while the
705   solid line is the sampled normalized squared error for the snow cover in FS.

706   Figure 14. Theoretical normalized squared error ($\sigma_{\bar{Z}}^2/\sigma_p^2$) as a function of the distance a from
707   the center of the area for square areas of side dimensions (L) between 10 and 80. Each curve
708   corresponds to an exponential decay (ν) between 0.1 and 5.

709   Figure 15. Theoretical and sampled normalized squared error ($\sigma_{\bar{Z}}^2/\sigma_p^2$) for the 5-point pattern
710   in Figure 12a over square areas of side dimensions (L) between 10.7 m and 79.1 m. The
711   separation distance (a) is varied from the center outwards. The solid line is the theoretical error
712   derived for an exponential decay exponent of 0.17 derived from the sampled correlation function
713   of snow depth in FS, while the solid red point markers are the sampled normalized squared error
714   for the snow cover in FS.

715   Figure 16. Theoretical normalized squared error ($\sigma_{\bar{Z}}^2 / \sigma_p^2$) for the N by N point pattern in
716   Figure 12b, and for areas of side dimension (L) between 10 and 80. The exponential exponent is
717   varied between 0.1 and 5.

718   Figure 17. Theoretical and sampled normalized squared error ($\sigma_{\bar{Z}}^2 / \sigma_p^2$) for the N by N point
719   pattern in Figure 12b, and over square areas of side dimensions (L) between 10.7 m and 79.1 m.
720   The solid black point markers are the theoretical error for an exponential decay exponent of 0.17
721   derived from the sampled correlogram of snow depth in FS. The dotted red lines with circle
722   markers are the sampled normalized squared error for the snow cover in FS.

723

724

References

725

726 Blöschl, G.: Scaling issues in snow hydrology, *Hydrol. Processes*, *13*(14-15), 2149-2175, 1999.

727 Chang, A. T. C., Kelly, R. E. J., Josberger, E. G., Armstrong, R. L., Foster, J. L., and Mognard,
728 N. M.: Analysis of ground-measured and passive-microwave-derived snow depth variations in
729 midwinter across the northern Great Plains, *J. Hydrometeor., 6*(1), 20-33, doi: 10.1175/Jhm-
730 405.1, 2005.

731 Cline, D., Yueh, S., Chapman, B., Stankov, B., Gasiewski, A., Masters, D., Elder, K., Kelly, R.,
732 Painter, T. H., Miller, S., Katzberg, S., and Mahrt, L.: NASA Cold Land Processes Experiment
733 (CLPX 2002/03): Airborne Remote Sensing, *J. Hydrometeor.*, *10*(1), 338-346, 2009.

734 Cressie, N.: *Statistics for spatial data*, 900 pp., John Wiley & Sons, Inc., USA, 1993.

735 Deems, J. S., Fassnacht, S. R., and Elder, K. J.: Interannual Consistency in Fractal Snow Depth
736 Patterns at Two Colorado Mountain Sites, *J. Hydrometeor., 9*(5), 977-988, doi:
737 10.1175/2008jhm901.1, 2008.

738 Grünewald, T., and Lehning, M.: Are flat-field snow depth measurements representative? A
739 comparison of selected index sites with areal snow depth measurements at the small catchment
740 scale, *Hydrol. Processes*, doi: 10.1002/hyp.10295, 2014.

741 Helfrich, K., Schöber, J., Schneider, K., Sailer, R., and Kuhn, M.: Interannual persistence of the
742 seasonal snow cover in a glacierized catchment, *J. Glaciol., 60*(223), 889-904, doi:
743 10.3189/2014JoG13J197, 2014.

744 Journel, A. G., and Huijbregts, C. J.: *Mining Geostatistics*, Academic Press, London, 1978.

745 Kronholm, K., and Birkeland, K. W.: Reliability of sampling designs for spatial snow surveys,
746 *Comput. Geosci.*, *33*(9), 1097-1110, 2007.

747 Lopez-Moreno, J. I., Fassnacht, S. R., Begueria, S., and Latron, J. B. P.: Variability of snow
748 depth at the plot scale: implications for mean depth estimation and sampling strategies,
749 *Cryosphere*, *5*(3), 617-629, 2011.

750 Matheron, G.: Application des méthodes statistiques à l'estimation des gisements, *Annales de
751 Mines*, *Dec*, 50-75, 1955.

752 Matheron, G.: Random functions, and their applications in geology, in *Geostatistics - A
753 colloquium*, edited by D. Merriam, pp. 79-87, Plenum Press, New York, 1970.

754 Melvold, K., and Skaugen, T.: Multiscale spatial variability of lidar-derived and modeled snow
755 depth on Hardangervidda, Norway, *Ann. Glaciol.*, *54*(62), 273-281, 2013.

756 Meromy, L., Molotch, N. P., Link, T. E., Fassnacht, S. R., and Rice, R.: Subgrid variability of
757 snow water equivalent at operational snow stations in the western USA, *Hydrol. Processes,
758 27*(17), 2383-2400, doi: 10.1002/Hyp.9355, 2013.

759 Mott, R., Schirmer, M., and Lehning, M.: Scaling properties of wind and snow depth distribution
760 in an Alpine catchment, *Journal of Geophysical Research: Atmospheres, 116*(D6), D06106, doi:
761 10.1029/2010jd014886, 2011.

762 Rice, R., and Bales, R. C.: Embedded-sensor network design for snow cover measurements
763 around snow pillow and snow course sites in the Sierra Nevada of California, *Water Resour.*
764 *Res., 46*, W03537, doi: 10.1029/2008wr007318, 2010.

765 Rodríguez-Iturbe, I., and Mejía, J. M.: Design of Rainfall Networks in Time and Space, *Water*
766 *Resour. Res.*, *10*(4), 713-728, 1974.

767 Schirmer, M., Wirz, V., Clifton, A., and Lehning, M.: Persistence in intra-annual snow depth
768 distribution: 1. Measurements and topographic control, *Water Resour. Res., 47*(9), W09516, doi:
769 10.1029/2010wr009426, 2011.

770 Shea, C., and Jamieson, B.: Star: an efficient snow point-sampling method, *Ann. Glaciol.*,
771 *51*(54), 64-72, 2010.

772 Skøien, J. O., and Blöschl, G.: Sampling scale effects in random fields and implications for
773 environmental monitoring, *Environ. Monit. Assess., 114*(1-3), 521-552, doi: Doi
774 10.1007/S10661-006-4939-Z, 2006.

775 Sturm, M., and Wagner, A. M.: Using repeated patterns in snow distribution modeling: An
776 Arctic example, *Water Resour. Res.*, *46*, 2010.

777 Trujillo, E., Ramirez, J. A., and Elder, K. J.: Topographic, meteorologic, and canopy controls on
778 the scaling characteristics of the spatial distribution of snow depth fields, *Water Resour. Res., 43*,
779 W07409, doi: 10.1029/2006WR005317, 2007.

780 Trujillo, E., Ramírez, J. A., and Elder, K. J.: Scaling properties and spatial organization of snow
781 depth fields in sub-alpine forest and alpine tundra, *Hydrol. Processes, 23*, 1575–1590, doi:
782 10.1002/hyp.7270, 2009.

783 Watson, F. G. R., Anderson, T. N., Newman, W. B., Alexander, S. E., and Garrott, R. A.:
784 Optimal sampling schemes for estimating mean snow water equivalents in stratified
785 heterogeneous landscapes, *J. Hydrol., 328*(3-4), 432-452, doi: 10.1016/J.Jhydrol.2005.12.032,
786 2006.

787 Yang, D. Q., and Woo, M. K.: Representativeness of local snow data for large scale hydrologic
788 investigations, *Hydrol. Processes, 13*(12-13), 1977-1988, doi: 10.1002/(Sici)1099-
789 1085(199909)13:12/13<1977::Aid-Hyp894>3.0.Co;2-B, 1999.

790

791